



2017

The Role of Black Hole and Neutron Star Interaction on the Dynamical Evolution of Dense Stellar Systems

Michael Pajkos
Butler University

Follow this and additional works at: <https://digitalcommons.butler.edu/ugtheses>



Part of the [Astrophysics and Astronomy Commons](#)

Recommended Citation

Pajkos, Michael, "The Role of Black Hole and Neutron Star Interaction on the Dynamical Evolution of Dense Stellar Systems" (2017). *Undergraduate Honors Thesis Collection*. 403.
<https://digitalcommons.butler.edu/ugtheses/403>

This Thesis is brought to you for free and open access by the Undergraduate Scholarship at Digital Commons @ Butler University. It has been accepted for inclusion in Undergraduate Honors Thesis Collection by an authorized administrator of Digital Commons @ Butler University. For more information, please contact digitalscholarship@butler.edu.

BUTLER UNIVERSITY HONORS PROGRAM

Honors Thesis Certification

Please type all information in this section:

Applicant Michael Anton Pajkos

(Name as it is to appear on diploma)

Thesis title The Role of Black Hole and Neutron Star Interaction on the
Dynamical Evolution of Dense Stellar Systems

Intended date of commencement 6 May 2017

Read, approved, and signed by:

Thesis adviser(s) B. L. May 4/21/17
Date

Reader(s) [Signature] 4/21/17
Date

Certified by _____ Date
Director, Honors Program

For Honors Program use:

Level of Honors conferred: University _____
Departmental _____

The Role of Black Hole and Neutron Star Interaction on the Dynamical Evolution of Dense Stellar Systems

A Thesis

Presented to the Department of History

College of Liberal Arts and Sciences

and

The Honors Program

of

Butler University

In Partial Fulfillment

of the Requirements for Graduation Honors

Michael Anton Pajkos

April 2017

Abstract

With the recent detection of gravitational waves from the Laser Interferometer Gravitational-Wave Observatory, or LIGO, a new realm of gravitational astrophysics has been opened. As the process of observing gravitational wave signals is still in its infancy, there is a need to provide gravitational astronomers with observable signatures in the electromagnetic spectrum. Hence, we explore the impact of solar mass black holes on the morphology of globular clusters. It has long been thought that due to high kick velocities from compact object gravitational interaction, Galactic age Globular Clusters are unable to retain black holes. Recent simulations, however, suggest that a significant population of black holes can be retained (Sippel & Hurley 2012, Rodriguez et al. 2016). We present the results from Fokker-Planck simulations of a time evolving Globular Cluster with an initial mass of $2.5 \times 10^6 M_{\odot}$. By exploring two different methods of IMF construction—evolved mass function and pure power-law—we are able to consistently determine their radial, density profiles with the introduction of $12 M_{\odot}$ black holes. Because of the efficiency of the Fokker-Planck code, we are able to explore parameter space as we observe how the globular cluster changes over initial mass functions with 0.1%, 1%, and 10% black holes retention rates—from initial black hole formation—and discover a significant impact on the cluster morphology between once the black hole population is on the order of 100. Moreover, we observe the segregation of black holes from the rest of the stellar members of the cluster and the influence of 3 body binary heating on the core of the segregated black hole sub-cluster. As we only address the initial ejection of black holes, and not their escape from the cluster over time, our future work will account for 3 body binary kicks that cause them to escape.

Table of Contents

Abstract.....	1
1. Introduction.....	3
2. Methods.....	7
3. Results.....	11
3.1. Evolved Mass Function	
3.1.1. 0.1% Black Hole Retention	
3.1.2. 1% Black Hole Retention	
3.1.3. 10% Black Hole Retention	
3.2. Pure Power-law	
3.2.1. 0.1% Black Hole Retention	
3.2.2. 1% Black Hole Retention	
3.2.3. 10% Black Hole Retention	
4. Conclusion.....	26
References.....	28

1. Introduction

Globular clusters are dense pockets of stars and compact objects, close to the age of Milky Way, that form from molecular clouds of gas. Because the initial mass of a star can vary, they can develop at different rates. Thus, at any point in time, a cluster can contain various kinds of objects, from early age main sequence stars to compact objects: white dwarfs, neutrons stars, or black holes.

Because the stars for a homogeneous cluster have identical origins, these clusters act as excellent laboratories for examining its differing characteristics, such as stellar evolution, kinematics, and mass segregation. More focused on the individual life cycle of a star, stellar evolution aims to examine the development of a star, over time. The kinematics of a cluster serve as a measure of the motion of its objects. And, in certain cases, mass segregation can occur as the more massive objects congregate to the center of the cluster and less massive ones disperse to larger radii.

As the stellar population of globular clusters can range from thousands to millions of stars, they often behave similar to a cloud of self-gravitating particles. Likewise, due to its similarity to a gas, the cluster will obey the equipartition of energy. The equipartition of energy is defined as the equal sharing of energy to each member of an entire system. Consequently, for a cluster of stars and compact objects, the cluster will experience mass segregation. When introduced into a globular cluster, the black holes form a cluster of their own, held up by 3 body binary heating, as the remainder of the cluster continues to evolve independently. In certain cases, globular clusters can experience core collapse. Core collapse describes the luminosity versus radius profile of a cluster. In the case of a core collapsed globular cluster, there exists such a high density of luminous objects that it

exhibits a power-law behavior. To begin our simulations, we expect that each cluster member of the cluster has equal velocity, a typical result of violent relaxation (Binney & Tremaine 1987). However, the velocity equipartition then quickly transitions to energy equipartition (Inagaki & Saslaw 1985; Murphy & Cohn 1988).

Before the age of space based telescopes, atmospheric turbulence severely inhibited resolving the inner core of globular clusters, thereby leaving little accurate information regarding the mass distribution of the cluster. The Hubble Space Telescope has been an invaluable resource regarding globular cluster kinematics, morphology, and stellar content because of its high resolving power. By resolving the nucleus of the cluster, astronomers are provided with extremely detailed information regarding the cluster's initial mass function (Murphy et al. 2011). The initial mass function describes the breakdown of each mass bin, by total percentage of the total cluster mass. This IMF is even well defined for core collapsed globular clusters. Because of the mass segregation of the stellar objects, the innermost region of the cluster is dominated by compact objects, thereby allowing us to constrain the upper end of the IMF. An effective mode to examining these distributions is through dynamical modeling of the cluster (Murphy et al. 2011).

Historically, stellar mass black holes are not incorporated into the mass function for multiple reasons. Possible birth kicks could eject them from the cluster (Dhawan et al. 2007). Likewise, according to the equipartition of energy, the more massive black holes would congregate to the cluster's center and quickly segregate from the rest of the cluster (Spitzer 1969; Watters et al. 2000). Furthermore, this central cluster could form

multiple binaries which could undergo three body interactions, causing them to eject from the cluster (Kulkarni et al. 1993; Sigurdsson & Hernquist 1993).

However, recent findings—consistent with both Monte Carlo and Fokker-Planck methods—suggest that as many as one-thousand $12 M_{\odot}$ black holes should be initially present in certain clusters (Rodriguez et al. 2016). Moreover, more observations in X-ray wavelengths continue to justify the presence of black holes within Galactic globular clusters (Strader et al. 2012). According to certain models, these black holes can range anywhere from a few solar masses to tens of solar masses, such as in M22 (Strader et al. 2012).

For a single population globular cluster, black holes form from massive stars. At the end of their time on the asymptotic giant branch, or AGB, they begin to fuse iron in their cores. Both the fusion and fission of iron is an endothermic process. Thus, the moment this fusion begins, the hydrostatic equilibrium of the stars are compromised. The higher pressure outside of the core forces the star to collapse on itself. The immense pressure causes the core to compress to the point where thermal pressure becomes insignificant, and the degenerate matter is held up according the Pauli Exclusion Principle.

$$\Delta x \Delta p \sim \frac{h}{2\pi}$$

The neutron degeneracy pressure causes the imploding envelope to ‘bounce’ and releasing a neutrino shock wave outwards. Although not every neutrino interacts with the matter of the star, those formed are on the order of 10^{42} , thereby causing an enormous

interaction with the stellar envelope. For stars massive enough, a collapsed core remains whose potential well is so deep, not even light can escape. Hence, a black hole is formed.

Consistent with the previous findings, as the mass difference between black holes and stellar neighbors increases, the more they decouple from the remaining stellar remnants of the cluster (Morscher et al. 2014). Moreover, after varying black hole initial retention from 0.1%, to 1%, to 10%, we notice little impact on the radial profile of the cluster from the black holes between 0.1% and 1% retention. A noticeable impact in the radial density plot of the stars is apparent once the black hole population is on the order of 100. These findings are consistent with the conclusions drawn from radial, luminosity profiles of certain clusters, such as M15, that claim there are very few black holes present, when a mass power-law profile exists (Murphy et al. 2015).

2. Methods

There are many methods to modeling systems with high numbers of elements—each with its own advantages. The two main types of modeling can focus on each element specifically or examine the system as a whole. The N-body method directly follows each element, individually, to track the evolution of the system. After the initial conditions are applied, the system will evolve forward slightly and then recalculate each element. The N-body method then repeatedly iterates, using small steps, until the evolution is complete. This method is effective at cataloging the trajectory of each star in the cluster. The drawback to N-body is that it requires vast amounts of computing power. In order to properly calculate the position of a single star, the code must consider its interaction with every other element in the cluster. Thus, with every new star introduced, the number of interactions grows nearly proportional to the square of the number of stars. In order to minimize computing time, scientists often turn to methods that consider the cluster as a whole.

Methods that consider distributions, instead of single particles, rely on statistics. In lieu of tracking individual bodies, statistical methods will observe how distributions of bodies evolve over time. Globular cluster numerical analysts often utilize two specific statistical methods: Monte Carlo simulations and the Fokker-Planck method. Monte Carlo simulations repeatedly draw random inputs in order to calculate a probability distribution of results. The Fokker-Planck method—by contrast—employs a differential equations to outline the evolution of stars within the cluster. The Fokker-Planck method can run quicker, compared to Monte Carlo simulations and is quicker than the N-body method by 100,000 (Heggie 2016).

We chose to utilize the Fokker-Planck model to examine our globular cluster. It is an improved version from the one utilized in Murphy et al. (1990). The equation behaves as follows:

$$\frac{\partial N(E)_i}{\partial t} = -\frac{\partial F_{E_i}}{\partial E}$$

where $N_i(E)$ represents the energy-space number density of the i th mass group. The energy term represents the total orbital energy of the orbiting compact objects and stars, combined. F_{E_i} represents the energy-space flux for the mass groups defined by

$$F_{E_i} = \sum_j (-D_{EEij} \frac{\partial f_i}{\partial E} - D_{Eij} f_i) - H_{Ei} f_i$$

where f_i represents the velocity-space distribution. D_{EEij} and D_{Eij} represent the flux coefficients and H_{Ei} is the three-body binary heating coefficient—dependent on stars of permitted energy E .

The aforementioned equations describe the dynamical evolution of the stars in the globular cluster. As we introduce stellar evolution, the distribution increases in complexity, by allowing for mass lost from each mass group. The concentration of stellar material with higher atomic numbers, or metallicity, is set to one one-hundredth the Solar value. Because the metallicity of a star has a significant effect on the radiation pressure exhibited, it has definite influence on stellar evolution.

The energy space of the cluster is divided into 100 discrete bins. As the Fokker-Planck is a statistical approach, the trajectories of the objects are independent of

direction. Thus, we can reduce the most general equation to a one-dimensional form, thereby expediting the calculations.

The initial parameters of the Fokker-Planck method are set by the Initial Mass Function—or IMF—of the cluster. This IMF is separated into 20 mass bins ranging from $12 M_{\odot}$ to $0.14 M_{\odot}$. Each of the 20 mass groups are segmented according to distributions of orbital energy. The IMF follows a three piece broken power-law outlined by Murphy et al. (2011) that is a best fit to the globular cluster M15. Similar to Murphy et al. (2011), we assume a neutron star retention rate of ten percent. Moreover, because it is poorly constrained, our present models assume a black hole retention rate of 0.1%, 1%, and 10%. As opposed to simply considering the dynamic evolution of each compact object, we also allow stellar evolution to occur. Thus, as the stars evolve off of the main sequence, and begin to increase in radius, their mass is eventually lost, whether it is due to planetary nebula formation, or supernova. In relation to the simulation, the lost mass is subtracted from each mass group as the model evolves, and the remnant masses are drawn from Hurley et al. (2000).

The timescale of the entire evolution of the cluster is comparable to the average lifetime of a main sequence star. As the Fokker-Planck method numerically solves over the entirety of the cluster age, the iterative step size must be adjusted depending on the stage of stellar evolution. Typically, a solar-like star will spend approximately 10 billion years on the main sequence. By contrast, its lifetime on the giant branch, or GB, and AGB are at least one order of magnitude less. Moreover, the GB and AGB portion of a star's life contain some of the most rapid changes in the star's radius and chemical composition. Because of the combination of short timescales and rapid stellar evolution,

the Fokker-Planck model incorporates an adaptive step size that will slow the code during rapid changes. Likewise, the code will increase the step size in periods of relatively slow stellar evolution to optimize run time and allow us to explore parameter space.

3. Results

In order to develop consistent results, we employ two different methods when developing our IMF. The first outlined is by evolved mass function. We generalize the work of Hurley et al. (2000) to incorporate black hole retention fractions. The second method is by mode of pure power-law. The power-law index was chosen to create a stable environment for the cluster to develop and kinematically evolve.

At certain points in the simulation we would obtain a numerical divergence. This is due to the construction of the energy and radial grid, which are subdivided into 100 and 115 bins, respectively. Post core collapse, the globular cluster will expand in size. As the cluster boundary grows to larger radii, it is lost off of the radial grid. Thus, once sufficient mass is lost, the Fokker-Planck recalculation steps can diverge. In all of the following cases, however, our cluster successfully reached core collapse before any numerical divergence occurred.

3.1 Evolved Mass Function

Bin	Stellar Mass (M_{\odot})	Mass Fraction	Type	Progenitor Mass (M_{\odot})
1	12.0	0.002	Black hole	50.0-22.0
2	1.44	0.010	Neutron Star	6.43-22.0
3	1.21	0.068	White Dwarf	4.00-6.43
4	0.95	0.133	White Dwarf	2.00-4.00
5	0.70	0.183	White Dwarf	1.00-2.00
6	0.57	0.063	White Dwarf	0.82-1.00
7	0.82	0.004	Red Giant	
8	0.80	0.021	Main Sequence	
9	0.73	0.067	Main Sequence	
10	0.62	0.096	Main Sequence	
11	0.52	0.062	Main Sequence	
12	0.44	0.042	Main Sequence	
13	0.38	0.032	Main Sequence	
14	0.32	0.032	Main Sequence	
15	0.28	0.031	Main Sequence	
16	0.24	0.031	Main Sequence	
17	0.20	0.030	Main Sequence	
18	0.17	0.030	Main Sequence	
19	0.15	0.028	Main Sequence	
20	0.13	0.021	Main Sequence	
21	0.11	0.015	Main Sequence	

Table 1—Initial mass function. (Evolved Mass Function) {1% initial retention—410 black holes present} Note, for the 0.1% and 10% initial retention case, the black hole mass fraction will vary by one order of magnitude.

Building on the work of Hurley et al. (2000), we create an evolved mass function in order to compare the performance of the pure power-law method. We incorporate black hole retention fractions, as well, to identify the three limiting cases when generating the IMF. We begin by displaying the central density plot, versus time, where the central density is in units of solar masses per cubic parsec and the time is a generalized code time. We then will examine the radial, density profile of the cluster at its initial state and at its maximum collapse. For the evolved mass function, we incorporate 21 mass groups, six of which are plotted: black holes, neutron stars, white dwarfs, red giants, and two masses of main sequence stars.

3.1.1 0.1% Black Hole Retention

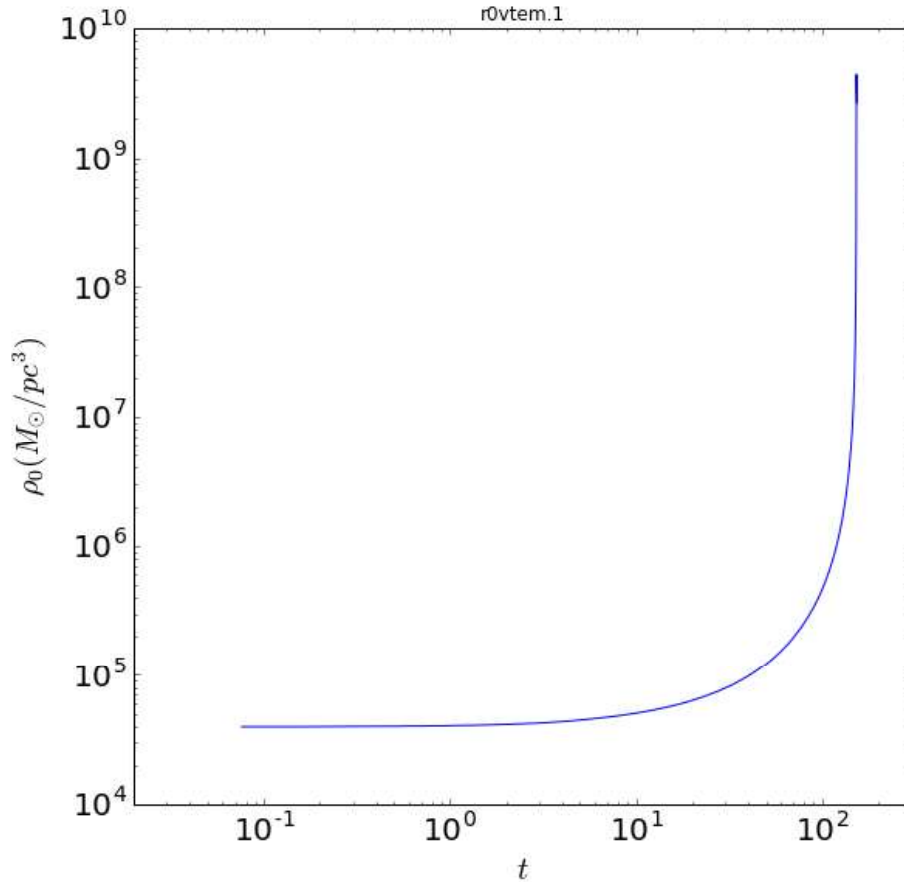


Figure 1—Central density versus time. (Evolved Mass Function)
 {0.1% initial retention—41 black holes present}

Our initial central density versus time plot is consistent with our later stellar evolution models in Section 3.2. Both occur close to the code time of 100, and have peaks within the same order of magnitude. The canonical core bounce is present as well.

With the introduction of the evolved mass function, neutron stars begin with a greater central density, as compared to the pure power-law case of stellar evolution. Likewise, the black holes, initially, occupy the lowest densities. For the core collapse case, we notice similar density peaks just under 10^9 solar masses per cubic parsec. Furthermore, as in the 0.1% power case, the core radius of the black holes marks the point of decline, with respect to density, for the remaining mass groups.

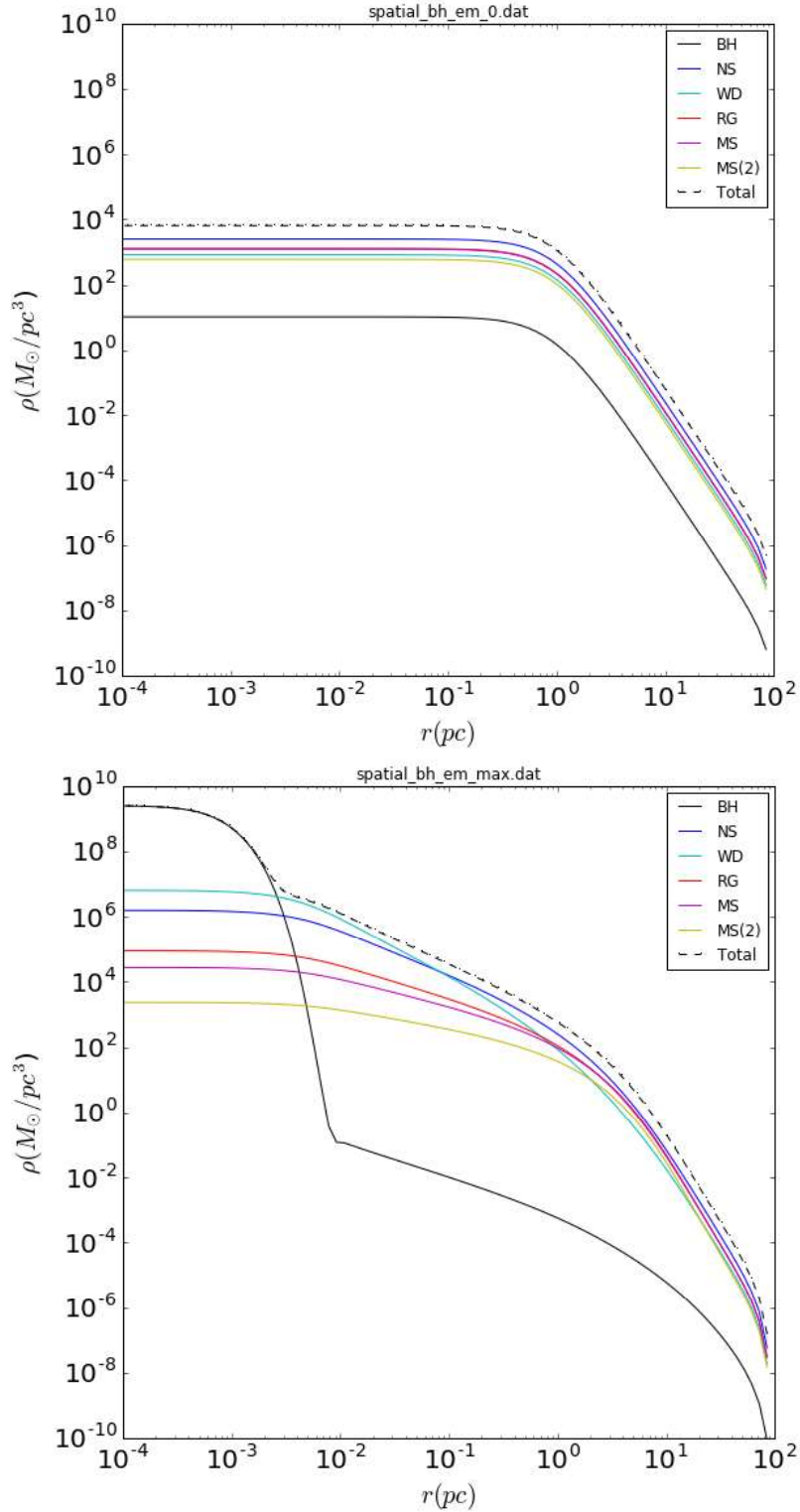


Figure 2—Radial density plot of the cluster before collapse [top] and at maximum collapse [bottom] (evolved mass function) {0.1% initial retention—41 black holes present}

3.1.2 1% Black Hole Retention

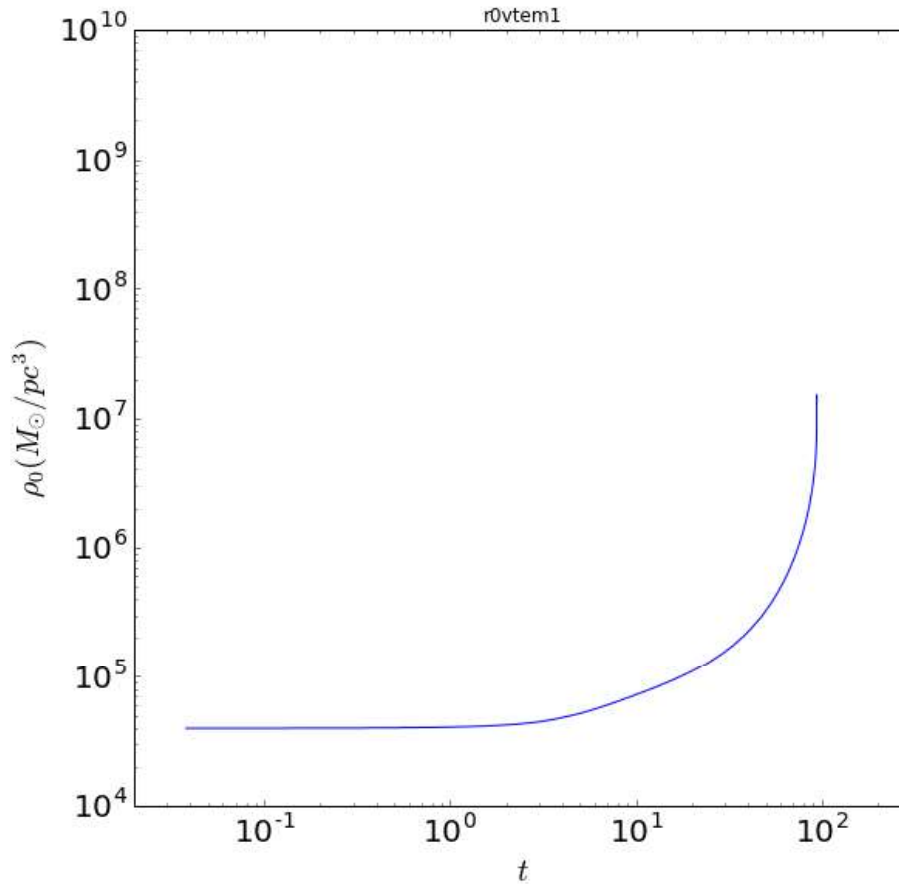


Figure 3—Central density versus time (evolved mass function)
 {1% initial retention—410 black holes present}

The evolved mass function central density versus time plot once again reaches a less dense collapse point. The beginning of the bounce can be seen near the maximum point of the graph, but—due to instabilities in our numerical model—soon after diverged. Thus, we plot all consistent points before the numerical divergence.

As expected the initial, central black hole density increases. Likewise, the initial densities of the remaining mass groups remain unchanged. The same mass segregation is beginning to form, as in the pure power-law, stellar evolution, case. Binary heating stays consistent as well. Moreover the larger black hole core radius, near 0.1 parsecs is indicative of the increasing relaxation time of the cluster.

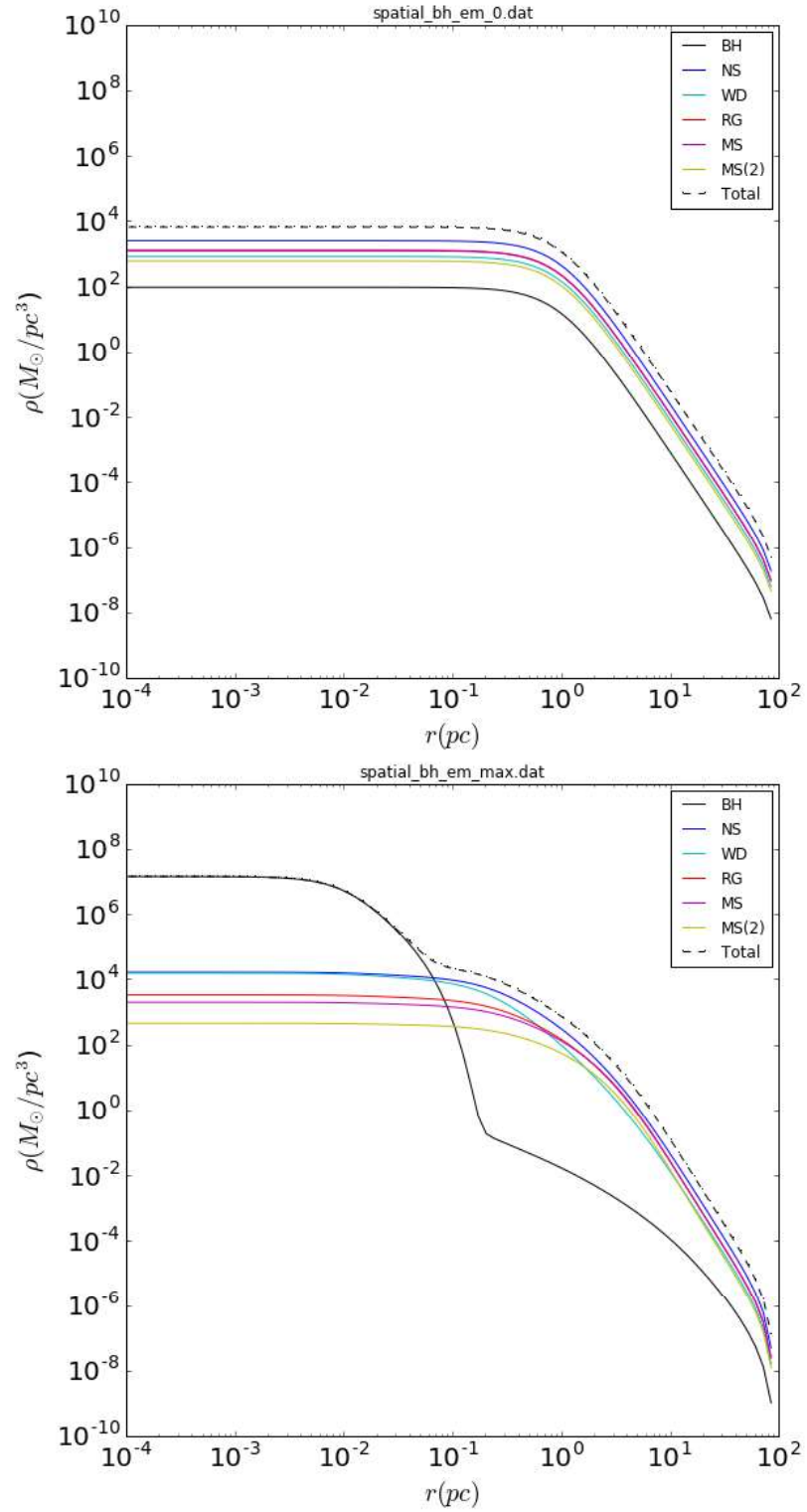


Figure 4—Radial density plot of the cluster before collapse [top] and at maximum collapse [bottom] (evolved mass function) {1% initial retention—410 black holes present}

3.1.3 10% Black Hole Retention

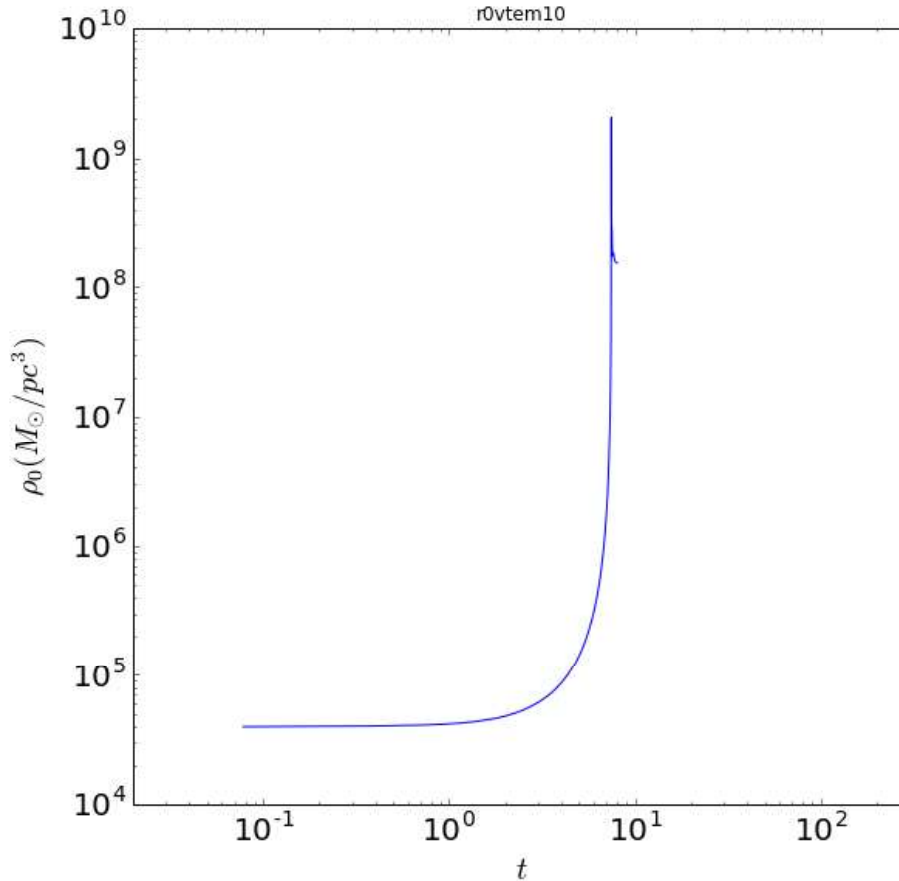


Figure 5—Central density versus time (evolved mass function)
 {10% initial retention—4100 black holes present}

As the black hole population has reached 4100, for the evolved mass function, the cluster has overcome the binary heating, forcing the cluster to collapse deeper and faster, by nearly one order of magnitude. This is due to the sub-cluster of black holes completely segregating from its stellar neighbors. Moreover, we notice how the power-law slope of the luminous stars has disappeared, compared to the lower retention percentages, in accordance with the predictions of Murphy et al. (2011).

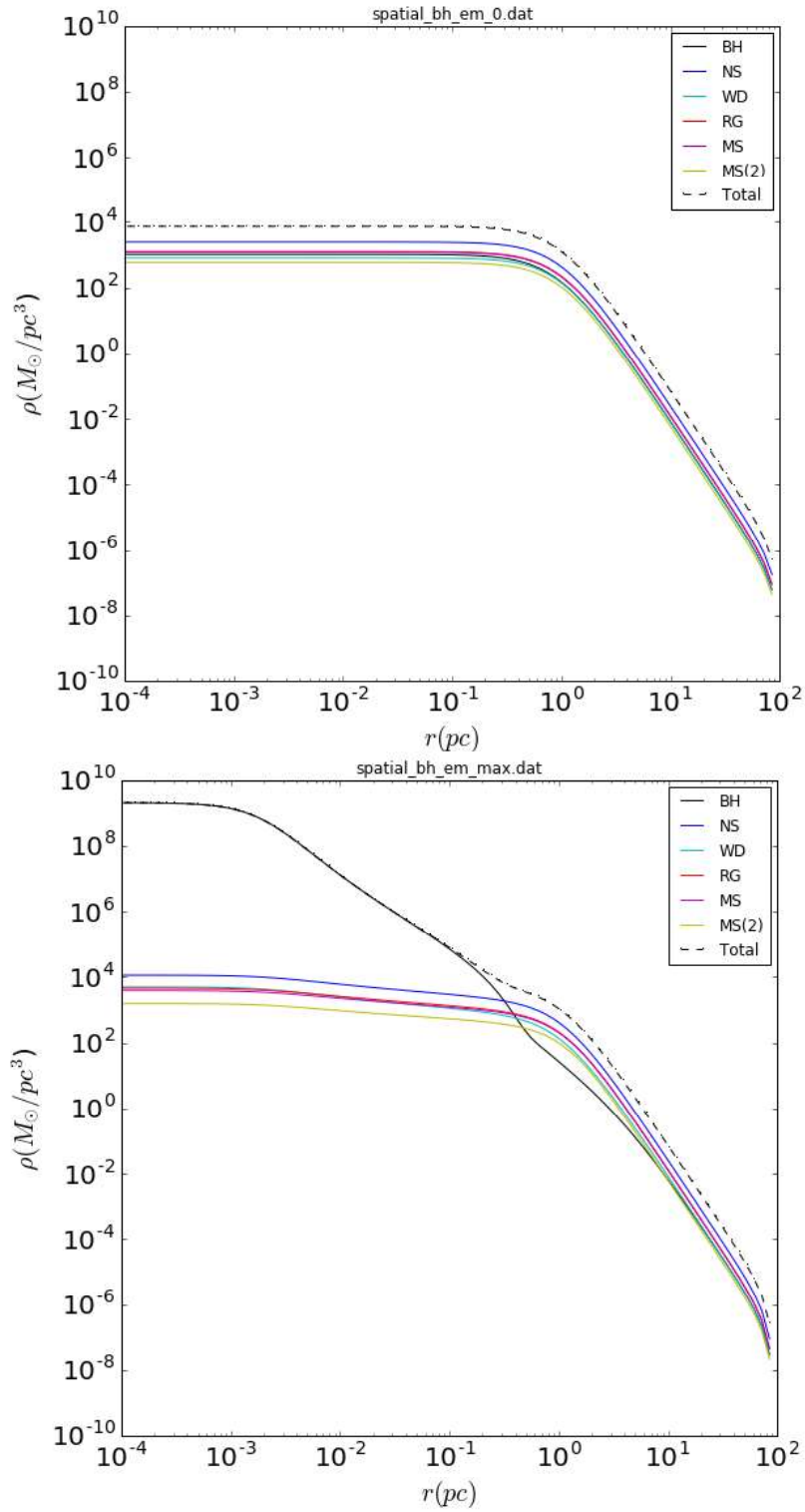


Figure 6—Radial density plot of the cluster before collapse [top] and at maximum collapse [bottom] (evolved mass function) {10% initial retention—4100 black holes present}

3.2 Pure Power-law

Our next models create a mass function with a constant power-law index of $x=1.2$, where $x=1.35$ is the Salpeter index. With the pure power-law method, we have the option of developing a self-generating IMF with or without stellar evolution. Thus, we consider both cases to see how the cluster without stellar evolution—closer to a cloud of self-gravitating ‘interacting particles’—and with—accounting for the kicks and mass transfer from exploding stars—can change over time. For the pure power-law, we incorporate 20 mass groups, with the same six mass groups plotted, as before: black holes, neutron stars, white dwarfs, red giants, and two masses of main sequence stars.

3.2.1 0.1% Black Hole Retention

When a black hole is formed from its parent supernova, a certain percentage are kicked from the cluster as the magnitude of their kinetic energy is greater than the magnitude of their gravitational potential energy, within the cluster. Thus, they are no longer gravitationally bound and can escape. As this percentage is poorly constrained, we begin exploring parameter space with a black hole retention rate of 0.1%. Figure 7 quantitatively displays the central density as a function of time.

Both models were run for differing amounts of time because of the heating and mass transfer that stellar evolution provides. Observe, in both cases, the core bounce that occurs as a result of the cluster overshooting hydrostatic equilibrium—forcing it to slightly re-expand. Likewise, observe the role that the stellar evolution plays as a factor to not only delay the initial core bounce, but cause a deeper collapse as well, by two orders of magnitude.

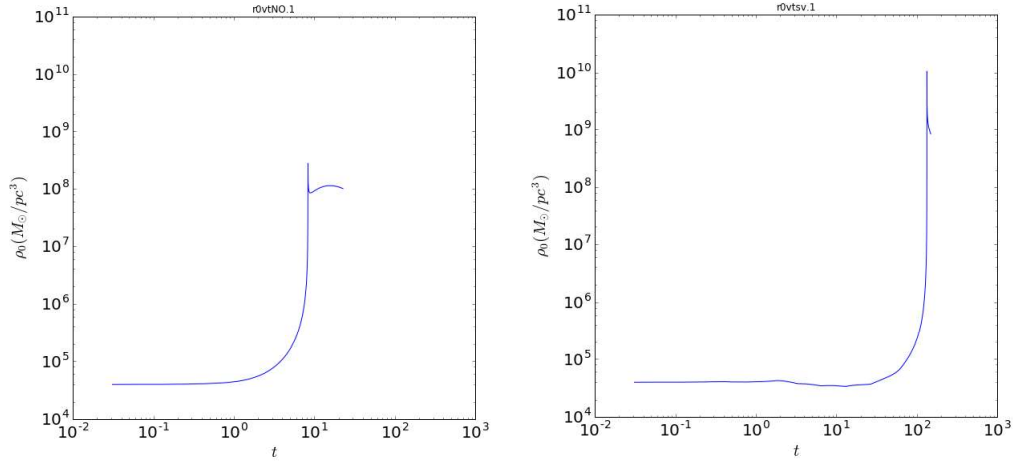


Figure 7—Central density versus time plot. No stellar evolution present [Left] Stellar evolution present [Right] {0.1% initial retention-3 black holes present}

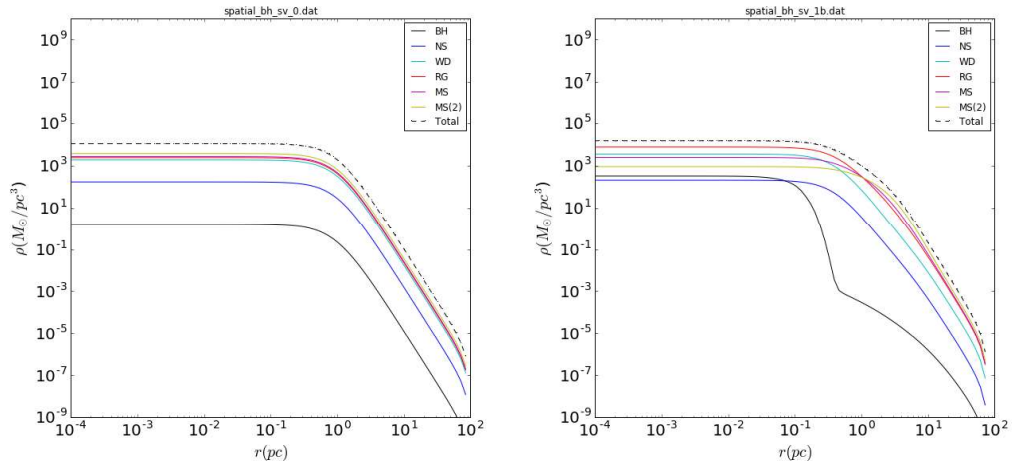


Figure 8—Radial, density plot of the initial cluster [Left] and at 1 billion years [Right] {0.1% initial retention-3 black holes present}

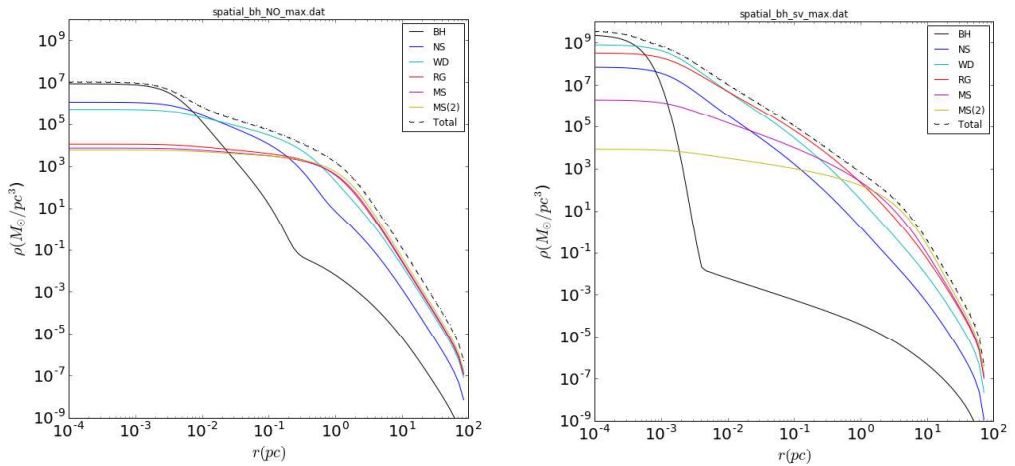


Figure 9—Radial, density plot at maximum collapse without stellar evolution [Left] and with stellar evolution [Right] {0.1% initial retention-3 black holes present}

Above displays the initial conditions of the cluster. As both cases, with stellar evolution and without, are derived from the same IMF, they are identical, thus we only plot one in Figure 8. As a point of clarity, although the initial retention percentages are equivalent for the evolved mass function, and pure power-law, they have different populations of black holes. This effect is a product of pure power-law construction of the IMF. As the index of $x=1.2$ preferentially favors less massive stars, compared to the evolved mass function, a smaller population of black holes will be present in the following models.

To the right of the initial cluster displays the evolution of the cluster at 1 billion years. The code utilized tracks time in years only for the stellar evolution case. Observe how the black hole group begins to segregate from the rest of the cluster. Moreover, as only 1 billion years is less than the relaxation time of the cluster, we observe the core radius of the black hole group near a radius of half a parsec.

Figure 9 depicts the cluster at maximum core collapse. The role of stellar evolution is apparent by increasing the density of the upper five, labeled mass groups by nearly two orders of magnitude. Moreover, at maximum collapse, the core radius of the black holes marks the point at which the remaining mass groups become less dense.

3.2.2 1% Black Hole Retention

With a retention rate increased by one order of magnitude, the mass fraction of the black hole group increases ten-fold. Hence, the increase in mass of the black hole group correspondingly decreases the mass of each of the remaining 19 mass groups. Hence we expect the black holes to have more of an influence on the cluster evolution.

As with the 0.1% case, stellar evolution drives the cluster into a deeper collapse. Interestingly, with the increase in black hole retention, the cluster collapses at the same time step as in the 0.1% case. Yet, with regards to maximum central density, the 1% case behaves differently. The maximum central density is slightly less when stellar evolution is present. More dramatically, for the stellar evolution case, the cluster's maximum central density is less by nearly two orders of magnitude. Physically, our models can be justified; as the amount of black holes increase, the central potential becomes increasingly negative, thereby creating a more tightly bound cluster. Hence, it is not subject to as extreme of a core bounce.

Compared to the 0.1% case, we observe an order of magnitude increase in the black hole maximum density. As the remaining mass groups contain the majority of the cluster mass, they only slightly decrease, to account for the black hole group increase.

As expected, the increase in black hole population of the cluster increases the maximum density of the black hole group. Moreover, this increase in maximum density is indicative of a more pronounced mass segregation. As with the initial parameters of the cluster, we notice little change to the maximum density of the remaining mass groups,

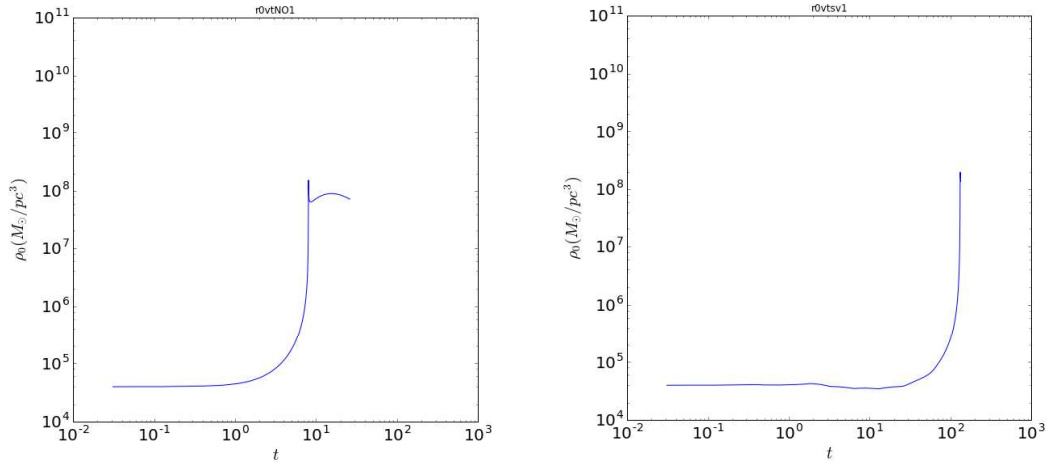


Figure 10—Central density versus time plot. No stellar evolution present. [Left] Stellar evolution present [Right] {1% initial retention-30 black holes present}

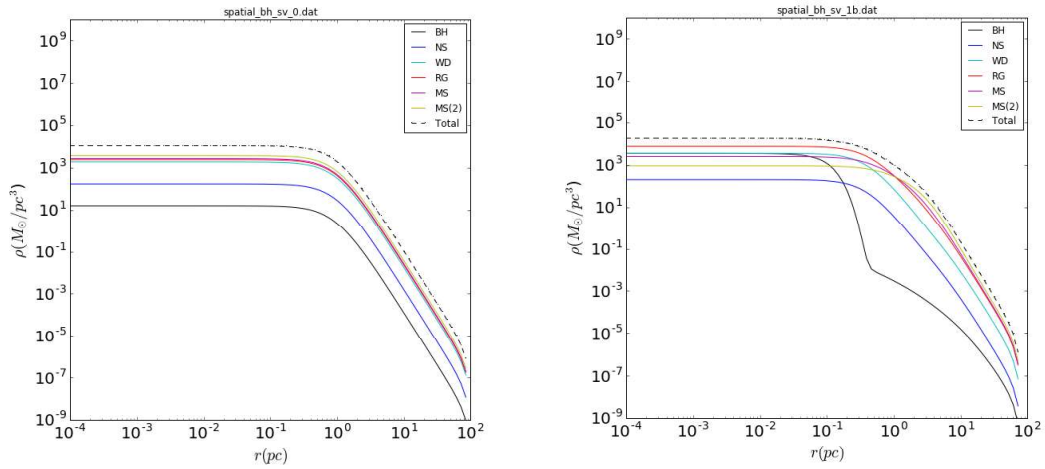


Figure 11—Radial, density plot of the initial cluster [Left] and at 1 billion years [right] {1% initial retention-30 black holes present}

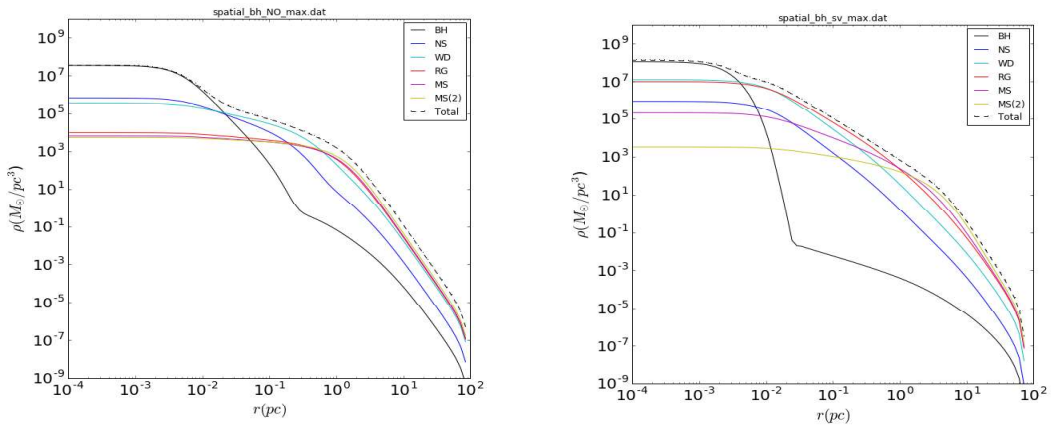


Figure 12—Radial, density plot at maximum collapse without stellar evolution [Left] and with stellar evolution [right] {1% initial retention-30 black holes present}

as well. We expect both the mass segregation and the remaining mass group influence to increase as the black holes represent even more of the cluster mass fraction.

As is consistent with the 0.1% case, the stellar evolution of the cluster drives a more extreme mass segregation—displayed by the steeper density versus radius slope—compared to the non-stellar evolution case. The maximum central density for both models is lower by nearly an order of magnitude for both cases. Although there is a higher population of black holes compared the 0.1% model, the role of black hole binary heating increases as their population increases.

Similar to the collision of gas particles in a pressurized environment, binary heating occurs as compact object binaries interact with a third, incoming compact object. After a three-body interaction, the lightest of the three objects will often be ejected. A portion of the gravitational potential energy of the original binary will be transferred to the kinetic energy of the lightest one, thereby ejecting it to larger cluster radii; thus resisting cluster collapse.

3.2.3 10% Black Hole Retention

Consistent with our predictions, the increase in black hole population to 10% further binds the cluster. In both cases, the maximum central density decreases, compared to lower black hole percentages. Likewise, the presence of a core bounce is still present, as is consistent through the 0.1%, 1%, and 10% cases.

At one billion years, with a more significant black hole population, the cluster segregation is furthered. Notably, after examining each of the black hole percentage models, the densities of the remaining mass groups remains relatively unchanged. Moreover, this clearly displays the role of black holes on globular cluster morphology. The larger the mass discrepancy between the black holes and stellar neighbors, the more the cusp of the stellar cluster is inhibited. Analogous to the 1 billion year model, binary heating has a significant impact on the cluster density for the 10% retention case, thereby causing a less dense core. Comparing the morphology of the maximum core collapse plot to the initial parameters, one can see a flatter initial slope between one one-thousandth and one one-hundredth of a parsec. By contrast, the 1% and 0.1% maximum core collapse plots are much steeper and have deviated from their initial radial density plots because their relaxation times are ~ 3 and 10 times less, respectively.

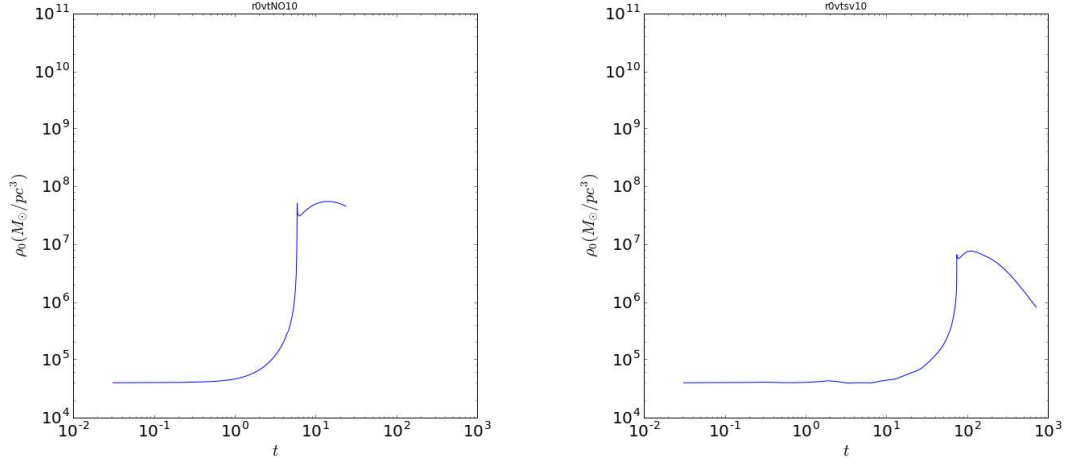


Figure 13—Central density versus time plot. No stellar evolution present. [Left] Stellar evolution present [Right] {10% initial retention-300 black holes present}

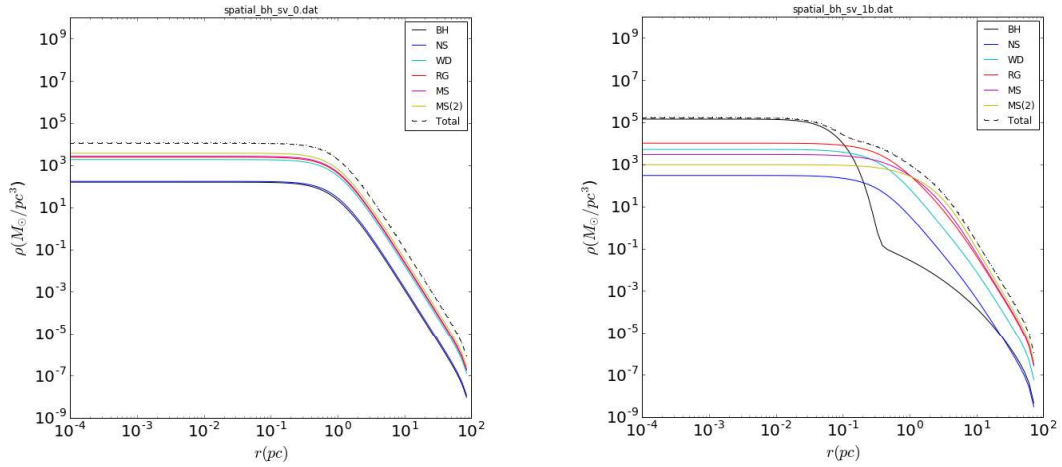


Figure 14—Radial, density plot of the initial cluster [Left] and at 1 billion years [right] {1% initial retention-300 black holes present}

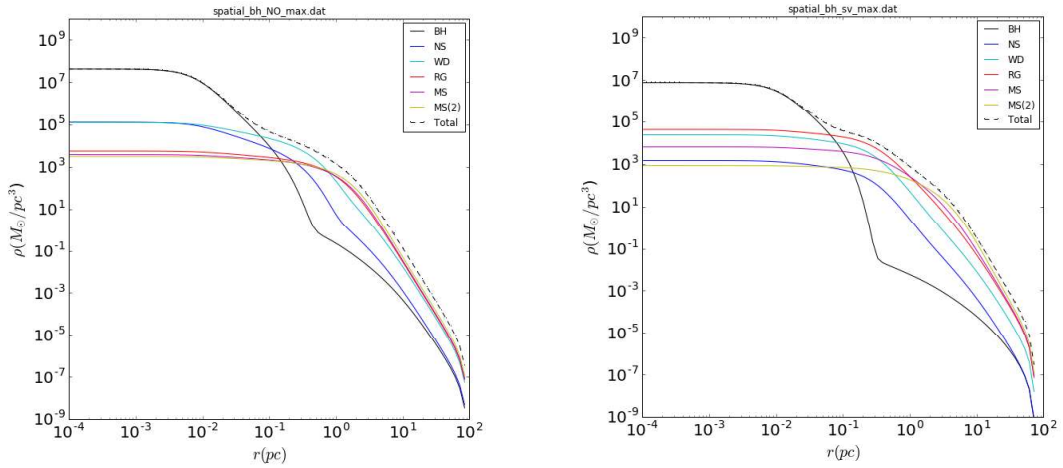


Figure 15—Radial, density plot at maximum collapse without stellar evolution [Left] and with stellar evolution [right] {10% initial retention-300 black holes present}

4. Conclusions

By employing two different methods of constructing initial mass functions, we have developed consistent results regarding cluster dynamics. By introducing 12 solar mass black holes into a cluster of 2.5 million solar masses, we have reaffirmed a variety of phenomena that occur with compact object dynamics and have theoretical predictions for the behavior of clusters that contain black holes. By inspecting the central density plots versus time, we have observed the typical core bounce that is seen with clusters of compact objects. By increasing the black hole retention fraction, for both the power-law and evolved mass function, it is apparent that binary heating dominates over the increased central potential, for black hole populations on the order of 100. Likewise, when introducing black holes into a dense stellar environment, as the black hole masses are nearly one order of magnitude greater than the next lowest mass group, they segregate from the stellar members of the cluster. Moreover, when the black hole population is on the order of 100, their gravitational interactions dominate, thereby inhibiting the cusp of the stellar cluster to develop. Hence, as gravitational astronomers continue the search for sources of emission from coalescing black holes, they will want to target clusters whose black hole population are on the order 100 or greater. These clusters will offer luminosity profiles that do not contain an observable power-law, thereby acting as reliable observational targets. Moving forward, as opposed to initially ejecting black holes and retaining a certain percentage, we plan to develop time evolving black hole loss mechanisms, in order to more accurately account for 3 body binary ejections.

5. Acknowledgements

I would like to thank my research advisor, Dr. Brian Murphy, for his guidance and permission to generalize his model. A special thanks for Dr. Gonzalo Ordonez for his advice. Likewise, thanks to the excellent support and preparation from the Butler University Physics and Astronomy department.

REFERENCES

- Dhawan, V., et al. 2007, **ApJ**, 668, 430
- Dull, J.D., Cohn, H.N., Lugger, P.M., 1997, **ApJ**, 481, 267-281
- Geiss, Brian B., “The Effect of Tidal Disruptions on Giant Stars in the Galactic Center” (2011). *Undergraduate Honors Thesis Collection*. Paper 123.
- Heggie, D.C., 2016, **Mem. S.A.It.** Vol. 87, 579
- Hurley, J. R., Pols O. R., Tout C. A., 2000, **MNRAS**, 315, 543
- Kulkarni, S. R., Hut, P., & McMillan, S. 1993, **Nature**, 364, 421
- Morscher, M., et al. 2015, **ApJ**, 800, 9
- Murphy, B.W., Cohn, H.N., Lugger, P.M., 2011, **ApJ**, 732, 67
- Rodriguez, C.L., et al. 2016, **MNRAS**, 463, 2109-2118
- Sigurdsson, S., & Hernquist, L. 1993, **Nature**, 364, 423
- Sippel, A.C., Hurley, J.R., 2012, **MNRAS**, 430, L30-L34
- Spitzer, L., Jr. 1969, **ApJ**, 158, L139
- Strader, J., et al. 2012, **Nature**, 490, 71
- Strader, J., et al. 2012, **Nature**, 777, 1
- Watters, W. A., Joshi, K. J., & Rasio, F. A. 2000, **ApJ**, 539, 331